Bull Volcanol (2013) 75:680
DOI 10.1007/s00445-012-0680-3

RESEARCH ARTICLE

Determination of the largest clast sizes of tephra deposits for the characterization of explosive eruptions: a study of the IAVCEI commission on tephra hazard modelling

Costanza Bonadonna · Raffaello Cioni · Marco Pistolesi · Chuck Connor · Simona Scollo · Laura Pioli · Mauro Rosi

Received: 2 August 2012 / Accepted: 18 December 2012 / Published online: 9 January 2013

Abstract The distribution of clasts deposited around a volcano during an explosive eruption typically contoured by isopleth maps provides important insights into the associated plume height, wind speed and eruptive style. Nonetheless, a wide range of strategies exists to determine the largest clasts, which can lead to very different results with obvious implications for the characterization of eruptive behaviour of active volcanoes. The IAVCEI Commission on Tephra Hazard Modelling has carried out a dedicated exercise to assess the influence of various strategies on the determination of the largest clasts. Suggestions on the selection of sampling area, collection strategy, choice of clast typologies and clast characterization (i.e. axis measurement and averaging technique) are given, mostly based on a thorough investigation of two outcrops of a Plinian tephra deposit from Cotopaxi volcano (Ecuador) located at different distances from the vent. These include: (1) sampling on a flat paleotopography far from significant slopes to minimize remobilization effects; (2) sampling on specified-horizontal-area sections (with the statistically representative sampling area depending on the outcrop grain size and lithic content); (3) clast characterization based on the geometric mean of its three orthogonal axes with the approximation of the minimum ellipsoid (lithic fragments are better than pumice clasts when present); and (4) use of the method of the 50th percentile of a sample of 20 clasts as the best way to assess the largest clasts. It is also suggested that all data collected for the construction of isopleth maps be made available to the community through the use of a standardized data collection template, to assess the applicability of the new proposed strategy on a large number of deposits and to build a large dataset for the future development and refinement of dispersal models.

Keywords Volcanic ash · Volcanic plumes · Field strategies · Tephra sedimentation · Particle characterization

Editorial responsibility: V. Manville

Electronic supplementary material The online version of this article (doi:10.1007/s00445-012-0680-3) contains supplementary material, which is available to authorized users.

C. Bonadonna (✉) · L. Pioli
Earth and Environmental Sciences Section, University of Geneva, Geneva, Switzerland
e-mail: Costanza.Bonadonna@unige.ch

R. Cioni
Dipartimento di Scienze Chimiche e Geologiche, Universita' di Cagliari, Cagliari, Italy

M. Pistolesi · M. Rosi
Dipartimento di Scienze della Terra, Universita' di Pisa, Pisa, Italy

C. Connor
Department of Geology, University of South Florida, Tampa, FL, USA

S. Scollo
Istituto Nazionale di Geofisica e Vulcanologia-sezione di Catania, Catania, Italy

Introduction

The definition of source parameters of explosive eruptions, including column height, mass eruption rate, total grain size distribution and eruption duration, is crucial to the hazard assessment of active volcanoes, which typically builds on the characterization of their eruptive history. In this context, the compilation of isopleth maps contouring the distribution of the largest clasts deposited around a volcano provides fundamental insights into: (1) the determination of column

height when no direct observations are available (e.g. Burden et al. 2011; Carey and Sparks 1986; Pyle 1989); (2) the definition of the eruptive style (e.g. Pyle 1989); and (3) the calculation of paleowind speed (e.g. Burden et al. 2011; Carey and Sparks 1986). The determination of the column height is extremely valuable also because it is used to derive information on the mass discharge rate (e.g. Mastin et al. 2009; Sparks 1986) and duration of eruptions (i.e. calculated from erupted mass and mass eruption rate). This paper summarizes the results of a field workshop associated with the third meeting of the IAVCEI Commission on Tephra Hazard Modelling carried out in Salcedo (Ecuador; January 16–18, 2006), with the main objective of assessing the best procedure to characterize the largest clasts of tephra deposits (also defined as "maximum clasts").

Recent advances in tephra modelling have shown that the column height of past eruptions cannot be easily constrained by inversion techniques applied to tephra loading on the ground (Connor and Connor 2006; Scollo et al. 2008) confirming the utility of the empirical approach first presented by Carey and Sparks (1986) and subsequently developed to account for variable wind profiles and to better describe uncertainties (e.g. Carey and Sigurdsson 1986; Burden et al. 2011). Nonetheless, various field investigations have shown the dependence of the results on the different clast measurements, averaging and sampling techniques used, confirming the need for a standardized strategy (e.g. Barberi et al. 1995; Biass and Bonadonna 2011). It is thus very important to understand the assumptions and limitations of the concept of "maximum clast" introduced by Walker and Croasdale (1971) and commonly used in the empirical approach of Carey and Sparks (1986). Standardization of the procedure for the characterization of the maximum clasts also becomes vital in reducing uncertainty in field sampling, and enables the eruptive parameters derived for different eruptions to be directly compared.

A standardized procedure acceptable to the scientific community needs to be developed based on a thorough testing and on the compilation of a large dataset, which will permit evaluation of the stability and reliability of selected procedures applied to a wide range of deposits. This paper aims at making the first step towards such a standardization (1) by directly comparing results of the most commonly used strategies to characterize the maximum clast, (2) by suggesting the testing of a new strategy that could provide more stable and representative results and (3) by inviting volcanologists to make all new data available to the scientific community to produce a large dataset for the assessment and development of a reliable standard procedure.

The 32 workshop participants worked directly on two outcrops to assess the variability of results due to individual measurements and the application of different techniques. Data were partially processed during the meeting and discussed with the whole group. Here, we present the main outcomes. The complete report, dataset and list of participants can be found at the website of the IAVCEI Commission on Tephra Hazard Modelling (http://dbstr.ct.ingv.it/iavcei/report1.htm and https://vhub.org/resources/870). Throughout the text, we will refer to this as the CTHM-Report.

Background

Isopleth maps were first introduced to the volcanological literature as descriptors of the sedimentological and dispersal features of tephra deposits (e.g. Walker and Croasdale 1971), which provide crucial insights into the energy of the dispersing and transporting system. Various physical models have been proposed to extract information on the dynamics and style of explosive eruptions from isopleth maps, such as the maximum height reached by the eruption column, the mass discharge rate (a proxy for the characteristic heat flux of the eruption) and the eruption classification (Carey and Sparks 1986; Pyle 1989; Wilson and Walker 1987). Each of these models presents several assumptions and caveats that are reviewed here.

Calculation of plume height

Even though a buoyant eruptive column is characterized by fluctuating vertical velocities, plume studies have shown that the time-averaged vertical speed can be represented by a Gaussian function that is symmetrical with respect to the plume axis (Turner 1979). From the comparison between this Gaussian function and the settling velocities of volcanic particles, Carey and Sparks (1986) defined a series of theoretical "envelopes" representing the ability of the erupting mixture to support clasts of a given density and size within the plume. Centreline velocities are typically sufficient to carry centimetre-sized clasts to the top of the eruption column of powerful eruptions, whereas larger clasts are deposited from the plume margins. When the particle settling velocity exceeds the plume upward velocity (characteristic of a given envelope), particles will leave the plume and eventually will deposit on the ground at a distance from the vent that depends on the clast features, on the column height and on the wind speed and direction. The method derives the column height and the wind speed by plotting the maximum downwind range versus the crosswind range measured on the isopleth contour lines describing the distribution of the largest clasts (lithic and pumice fragments) deposited on the ground. Validation with radar, satellite and meteorological data was carried out for the 18 May 1980 eruption of Mt. St. Helens (Carey and Sparks 1986) and with the 1991 eruption of Pinatubo (Rosi et al. 2001). Some of the empiricism characteristics of the method of Carey and

Sparks (1986) have been addressed by Burden et al. (2011), who have better quantified model uncertainties.

Vertical velocity Plume vertical velocity in the model of Carey and Sparks (1986) is determined for sustained plumes between 7 and 43 km high. As a result, such a model should only be applied to subplinian and Plinian deposits. Woods (1988) showed that large plumes might be characterized by superbuoyancy, in which case the vertical velocity profile is not monotonic as assumed by Carey and Sparks (1986). This also results in a non-uniform lateral decrease of the ascent velocity inside the column, and hence in a non-concentric distribution of the isovelocity shells (as defined by Carey and Sparks, 1986), which describe the ability of the plume to carry clasts of a given size and density at a certain height. Effects of superbuoyancy can be addressed by describing plume dynamics based on numerical models, such as Woods (1988) (e.g. Burden et al. 2011). In addition, the choice of the contour lines to use for the calculation significantly affects the plume height determination. For example, both Papale and Rosi (1993) and Di Muro et al. (2008) showed that the coarsest isopleth lines result in lower columns than the 0.8- and 1.6-cm isopleth lines. This was confirmed by Biass and Bonadonna (2011) who showed that plume heights of two Cotopaxi eruptions (Ecuador) derived with the model of Carey and Sparks (1986) were 10 % lower using the 3.2- and 6.4-cm contours than those based on the 0.8- and 1.6-cm isopleth lines.

Wind profile The vertical wind profile considered in Carey and Sparks (1986) is from Shaw et al. (1974) and assumes a maximum velocity (5–30 m/s) at the tropopause level (considered fixed at 11 km for all latitudes). The wind velocity then decays linearly to zero at ground level and is 0.75 the maximum value above the tropopause. However, wind profiles are typically more complex and may vary during the course of an eruption. As an example, Carey and Sigurdsson (1986) modified the wind profile used in Carey and Sparks (1986) in order to account for a direction inversion above the tropopause that occurred during the 1982 eruption of El Chichon. In addition, the tropopause height varies by up to 8 km between high and low latitudes, affecting the wind-profile structure. Wind variability has also been analysed as a source of uncertainty in the work of Burden et al. (2011).

Column height and mass eruption rate The plume height derived using the method of Carey and Sparks (1986) represents the maximum height reached during a given eruption because it is based on the distribution of the largest clasts found in the deposit. Therefore, the mass eruption rate determined using this method also represents a maximum value. In order to assess the fluctuation of plume height and mass eruption rate at different times, isopleth maps are often compiled for different stratigraphic levels (e.g. Vesuvius 79 AD eruption; Carey and Sigurdsson 1987). Unfortunately, equivalent stratigraphic levels within the same fallout deposit are normally difficult to distinguish in distal areas, being traceable with distance from vent only when the tephra deposit is characterized by distinct markers.

Eruption classification

Pyle (1989) introduced a plot to classify volcanic eruptions as an alternative to the classification of Walker (1973). Such a plot is based on the concept of the thickness half distance (b_t) and the half distance ratio (b_c/b_t) introduced by Pyle (1989), where b_c is the maximum clast size half-distance. Such a diagram is, in theory, easier to apply than the diagram of Walker (1973) because it does not require any grain size analyses. However, the classification of Pyle (1989) is strongly sensitive to the choice of clast-averaging technique, e.g. the layers 3 and 5 of Cotopaxi volcano (Ecuador) can be classified as either Plinian or subplinian when different averaging techniques are considered (Biass and Bonadonna 2011).

Methods for largest-clast (maximum-clast) assessment

The choice of the averaging technique for the assessment of the largest clasts is probably the most controversial issue in applying the method of Carey and Sparks (1986). Scientists calculate "maximum clasts" in different ways and have also applied different techniques to different deposits. Suzuki et al. (1973) showed how the average of the maximum axis of the 10 largest clasts over a 1-m^2 outcrop area is comparable to the 1 % coarsest percentile of the grain size of a given outcrop, whereas Sparks et al. (1981) showed that the geometric mean of the three axes of the five largest pumice clasts is 1.5 times larger than the 1 % coarsest percentile. After reviewing 47 cases from the volcanological literature, Biass and Bonadonna (2011) presented the statistics for the most common methods used (Fig. 1): (1) the average of the largest axis of the five largest clasts (30 %), (2) the average of the largest axis of the three largest clasts (19 %) and (3) the average of three axes of the five largest clasts (19 %). Regardless of the number of clasts considered, the three axes were most commonly averaged based on the arithmetic mean (28 %), while a 0.5-m^2 sampling area was used in 15 % of the cases, even though specifications about the sampling are rarely mentioned (64 % of the cases). The application of different techniques generates different isopleth maps and therefore can significantly affect the determination of column height and wind speed using the method of Carey and Sparks (1986). Barberi et al. (1995) have shown how using the average of the maximum axis of the three largest clasts collected from a 2-m long exposure and excavating 5 cm of the deposit (0.1-m^2 horizontal area)

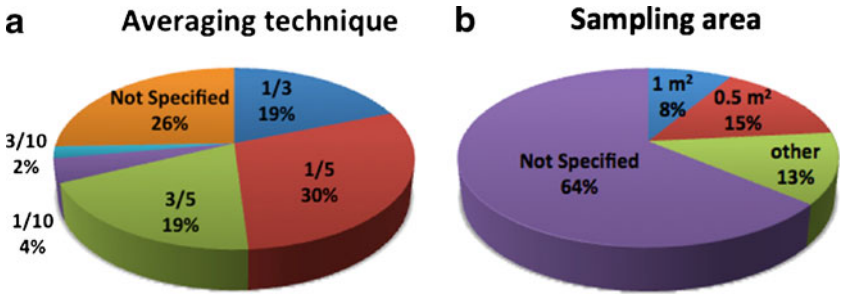

Fig. 1 Most common methods used to determine the maximum clast presented by Biass and Bonadonna (2011) for **a** averaging technique described in Table 1 and **b** sampling area used

underestimates the crosswind range by 20–40 %, compared with an isopleth map compiled by averaging the maximum axis of the five largest clasts sampled over a 0.5-m^2 horizontal area.

Lithic or juvenile fragments At a single locality, the size of pumice clasts is typically two to five times larger than that of associated lithic fragments, due to their lower density (Carey and Sparks 1986), with the ratio of pumice to lithic diameter becoming progressively smaller as the vent is approached due to preferential breakage of large pumices (Sparks et al. 1981). In fact, juvenile clasts (both pumice and scoria fragments) tend to be smaller than their original size because they commonly break upon impact with the ground, and breakage is more efficient for coarse grains (Sparks et al. 1981). Lithic clasts are typically less breakable (unless strongly altered) and therefore lithic isopleth maps have been generally preferred when applying the method of Carey and Sparks (1986). However, lithic clasts may be strongly non-spherical and could also have vesiculation that lowers their density (e.g. vesiculated lava fragments). These lithic clasts should not be considered in the calculation. In addition, some tephra deposits do not contain many lithic fragments and/or the lithic fragments are difficult to distinguish from the juvenile clasts. This is a common problem in basaltic explosive deposits (e.g. Etna 122 BC Plinian eruption; Coltelli et al. 1998), but can be overcome in cases where dense juvenile clasts are present. Although dense juvenile and lithic fragments are often difficult to distinguish, dense juvenile clasts can be used in place of lithics, as they less frequently break upon impact with the ground and the density is similar to that of the lithic clasts.

Oversize clasts When collecting the largest clasts at a given outcrop, it is common to find a clast that is significantly larger than the rest of the population. Do we disregard such a clast or can we consider it as representative of eruption processes? Several statistical methods are available to determine whether a given clast belongs to a given population. Two of the most common methods are the method of Dixon (1950) (typically used to determine outliers of small populations; Appendix A) and the boxplot method (Tukey 1977). Advantages and limitations of these methods are presented in "Detection of outliers" section.

The IAVCEI workshop exercise

The exercise was performed on two outcrops of a massive andesitic pumice layer produced by a Cotopaxi eruption around 800 years ago (i.e. top unit of layer 3 in Barberi et al. (1995), defined here as "yellow top"). The two outcrops were selected in medial (outcrop 1; 13 km from the vent; thickness= 14 cm; Mdϕ=−2.9; $\sigma\phi$=1.4) and distal area (outcrop 2; 22 km from the vent; thickness=5 cm; Mdϕ=−1.5; $\sigma\phi$=1.4) in order to assess the influence of grain size on the characterization of the maximum clast (Fig. 2). In the exercise, we assessed the effects of the following parameters on the evaluation of the maximum clast: (1) measurement of clast axis; (2) detection of outliers; (3) comparison amongst different averaging techniques and different collection strategies; (4) variability of measurement within a given outcrop; and (5) effects of the size of sampling area.

Measurement of clast axis

Particle size and shape analysis starts with the measurement of the three mutually perpendicular characteristic lengths (here defined as axes). However, the determination of these three axes is not unique, as each operator can follow a different approach to the measurement. Two different basic approaches exist for the measurement of these lengths (Fig. 3). In both, the shortest axis (c) is defined as the shortest distance between two opposite corners of the clast. In the maximum ellipsoid approach (Yuzyk and Winkler 1991), the longest axis (a) is defined as the longest distance between two opposite corners of the clasts along a plane perpendicular to c, and the intermediate axis (b) is the distance taken perpendicular to both c and a. In the minimum ellipsoid approach (Gordon et al. 1992), the intermediate axis (b) is identified as the shortest distance between two opposite corners of the clast along a plane perpendicular to c and the longest axis a is subsequently defined as the distance taken perpendicular to both c and b axes, and, thus, it is not necessarily the longest distance between two opposite corners of the particle. The differences in the longest and shortest axis definitions become irrelevant for smooth ellipsoidal shapes, but are significant for rhomboidal shapes. We have investigated the variability of measurement by

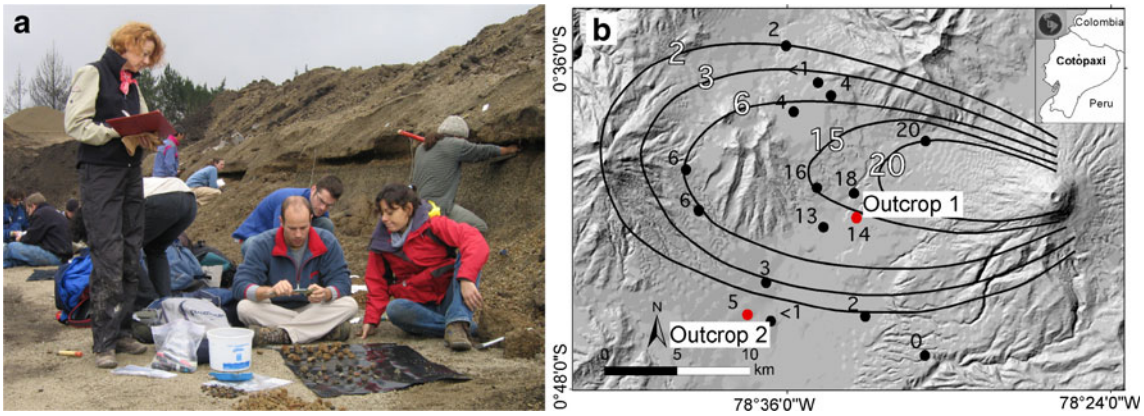

Fig. 2 **a** Workshop participants working on the 0.5-m^2 areas at outcrop 1. **b** Isopach map (centimetre) of "yellow top" of layer 3 considered in our exercise. The location of outcrops 1 and 2 is indicated with *red circles*

having seven people measure three axes of the same 10 lithic clasts. Figure 3 shows the associated arithmetic mean and standard deviation. The difference between the geometric mean (determined from the measured axes) and the diameter of the equivalent sphere (determined after measuring the volume of the same particle by immersion technique) is between 0.2 and 18.5 %, with an average difference per person between 2 and 12 %. The lowest percentage difference was obtained by the investigators that approximated the clast considering the minimum ellipsoid (i.e. solid lines in inset of Fig. 3). The diameter of the equivalent sphere of our analysed particles is typically smaller than the diameter based on the geometric mean of the particle. In addition, given that the measurements of the largest clasts are used for application in models that are based on the assumption of spherical particles (e.g. Carey and Sparks 1986), it is important to assess the equidimensionality of clasts to avoid large discrepancies with the model assumptions. Both pumice and lithic clasts from our two outcrops show a scatter of shape factor F between 0.3 and 0.95 (with $F=(b+c)/2a$ as defined in Wilson and Huang (1979)) with respect to the geometric mean, which represents the diameter of a sphere with the same volume as the ellipsoid with the same axes as the measured clast (c.f. Fig. 23 of CTHM-Report). In addition, the working sphericity of Aschenbrenner (1956) of pumice and lithic clasts of the two outcrops is between 0.62 and 0.95, which includes the value of 0.89 used by Burden et al. (2011) as an alternative to the spherical assumption.

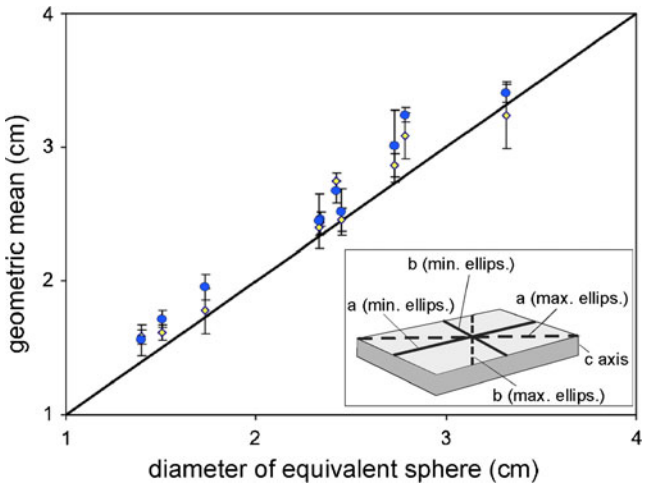

Fig. 3 Mean and standard deviation of two sets of clast measurement data based on the assumption of minimum (*yellow diamonds*) and maximum ellipsoid (*blue circles*), respectively. The *straight line* indicates the 1:1 relation. The *inset* shows the two different basic approaches for the measurement of the three axes of a clast based on the maximum (*dashed lines*) and minimum (*solid lines*) ellipsoid. See text for more details

Detection of outliers

The presence of "oversize" clasts (i.e. size outliers) is a delicate issue in the assessment of the largest clasts. Several methods for treating outliers exist in the statistical literature (e.g. Barnett and Lewis 1998) but no standard method is currently used in tephra studies. Data outliers can be due to inherent variability (e.g. could reflect the distribution in the extreme tail), measurement error or execution error (Barnett and Lewis 1998). Given that clast measurements are typically done in the field, the possibility of measurement error is considered low (assuming that the detection of outliers is first done visually). In contrast, execution error (imperfect collection of the data) and inherent variability (natural variation of the population) are two possible causes that need to be carefully analysed. Even when the outlier values are perfectly legitimate, they can cause calculation anomalies if they lie outside the range of most of the data. As a result, different strategies have been proposed to deal with outliers, mainly accommodation (not requiring outlier identification) or rejection of outliers (requiring the application of detection tests).

There are several ways to accommodate outliers to mitigate their effects (e.g. nonparametric analysis, data transformation). Deletion can be considered only as a last resort and only if they significantly affect the final results. Here, we discuss the application of two methods commonly used to detect outliers: boxplot (Tukey 1977) and Dixon's test (Dixon 1950). The boxplot method is a convenient way to describe a population of values without making any assumptions on the statistical distribution and identifies potential and problematic outliers, particularly for large datasets. The Dixon's test is more appropriate for small datasets but has been shown to be particularly effective when the data come from a normal distribution (Chernick 1982) (Appendix A). A sensitivity analysis was carried out on a sample of pumice clasts collected at outcrop 1 (0.1-m^2 area α, see CTHM-Report for more details). Results show how both the boxplot and the Dixon's test are affected by the size of the sample, identifying different outliers for 5-, 10- and 20-clast samples. A better method to deal with outliers is the accommodation based on the use of the median, which is less affected by the presence of extreme values with respect to the arithmetic mean. This is an example of accommodation strategies using a robust parameter. The median values calculated for the 20-clast samples showed the highest stability with respect to the 5- and 10-clast samples, suggesting that the use of large samples is more appropriate to deal with outliers even when a robust parameter such as the median is used.

Comparison amongst different averaging techniques and different collection strategies

In this section, we report the results of the measurements of the largest pumice and lithic clasts at outcrops 1 and 2, for different sampling areas, using both the "specified-area" and "unspecified-area" collecting strategies and applying different averaging techniques (Tables 1 and 2). In particular, specified area refers to the strategy in which the sampling is carried out throughout the whole thickness (depth) of the fallout bed by digging a fixed sedimentation (horizontal) area defined by the outcrop width and length (e.g. 0.1 and 0.5 m^2; Table 2 and Fig. 4). The sampling associated with the unspecified-area strategy is mainly carried out on the external (generally vertical) surface of the outcrop with no fixed width and length; although faster, it is often based on a smaller volume of investigated material.

Specified-area sections (0.1 and 0.5 m^2)

A total of 20 pumice and 20 lithic fragments were collected at outcrop 1 in five areas of 0.1 m^2 each (α to ε) and eight areas of 0.5 m^2 each (A to H) (Table 2). The technique of averaging the largest axis of three and five clasts gives very different results compared with the techniques that consider the arithmetic and geometric mean of the three axes (Figs. 5 and 6). A population of values resulting from the average of the maximum axes (1/3 and 1/5) and a population of values that average the arithmetic and geometric mean of the three axes (A3/3, A3/5, G3/5, A3/10, A3/12) can be identified for all plots. Furthermore, values of maximum clast associated with the 0.5-m^2 sections are more stable (i.e. show less variability) and corresponding standard deviations are more homogeneous than those associated with the 0.1-m^2 sections (Fig. 5a–b). Finally, the values of maximum pumice clast sizes are clearly more variable than the values of maximum lithic clast sizes (Fig. 5c). Twenty pumice and 20 lithic clasts were also collected at outcrop 2 in 10 areas of 0.1 m^2 each (A to J) (Table 2). The effect of the size of sampling area was investigated by coupling the results of sequential areas of 0.1 m^2 to obtain nine areas of 0.2 m^2 each (Fig. 5d–e). For outcrop 2, which is characterized by a smaller grain size than outcrop 1, values collected over an area of 0.2 m^2 are more stable and seem to characterize quite well the maximum clast size of the outcrop (lithic values are shown in Fig. 5d–e). However, a detailed analysis of all possible combinations of the 0.1-m^2 areas shows a significant fluctuation of values (see Appendix F of CTHM-Report for more details).

Collection strategy: unspecified area (section length: 2 and 4 m)

Twenty pumice and 20 lithic fragments were also collected at outcrops 1 and 2 to assess the sampling of unspecified areas (Table 2). Here, we present only the results of the lithic clasts of outcrop 1 to show the strong influence that the outcrop length has on the application of the unspecified-area collection, with the lowest values given by clasts collected in the shortest outcrops (i.e. A and B; Fig. 5f). Similar results were obtained for pumice and lithic fragments of both outcrops 1 and 2, with no lithic clasts being found at the 0.5-m sections of outcrop 2 (see CTHM-Report for more details).

Effects of the size of sampling areas with respect to different averaging techniques

The discrepancies between different averaging techniques vary from 100 to −65 %, with the 1/3 technique resulting in values about 70 % higher than the G3/5 technique for both outcrops (Fig. 6a–b). In contrast, the difference between different averaging techniques is mostly unaffected by the sampling area (Fig. 6c).

Table 1 Description of all averaging techniques used to determine the largest clasts in all areas and all outcrops

Averaging technique	Description
1/3	Arithmetic average of maximum axis of 3 clasts
1/5	Arithmetic average of maximum axis of 5 clasts
A3/3	Arithmetic average of arithmetic mean of the 3 axes of 3 clasts
A3/5	Arithmetic average of arithmetic mean of the 3 axes of 5 clasts
G3/5	Arithmetic average of geometric mean of the 3 axes of 5 clasts
A3/10	Arithmetic average of arithmetic mean of the 3 axes of 10 clasts
A3/12	Arithmetic average of arithmetic mean of the 3 axes of 12 clasts

Variability of measurement within a given outcrop

An important aspect of any data collection is the reproducibility of measurements. We have investigated the reproducibility of the evaluation of the largest clasts within the same outcrop for: (1) outcrops 1 and 2; (2) pumice and lithic clasts; and (3) different averaging techniques. Variability is investigated by plotting an empirical survivor distribution of each of the 20-clast samples collected at each individual section of the same outcrop. The survivor function describes the probability P that a clast is larger than a given value (Fig. 7; see CTHM-Report for the complete dataset). In detail, clast size is sorted in ascending order, x_1, x_2, …, x_N, where N is the number of clasts, then:

$$P_i = 1 - \frac{i}{N} \text{ for } 1 \leq \text{i} < \text{N} \quad (1)$$

The large variability of the values of the largest clasts is obvious in most plots, and in particular for the pumice plots. This is likely due to variable vesiculation and density (density of 20 pumice and lithic clasts varies between 300 and 1,200 kg/m^3 and 2,600–3,100 kg/m^3, respectively; cf. Table 13 of CTHHM-Report). Lithic measurements are affected by smaller variations than pumices, and variability seems to increase below the nearest-rank 50th percentile (i.e. the smallest of the 10 largest clasts) (Fig. 7b). Percentage differences between the 50th and the 5th percentile vary between 27 and 41 for the maximum axis technique and 29 and 37 for the geometric mean technique for both outcrops (Table 3). The advantage of considering the median of a large sample was already discussed in "Detection of outliers" section as an alternative accommodation strategy that better deals with outliers. The nearest-rank 50th percentile provides similar advantages as the median but it is preferred because it does not require the assumption of a continuous distribution.

Effects of the size of sampling areas

The effect of sampling area (and hence volume) on the evaluation of the maximum clast was tested by investigating the stability of results for the two outcrops for different collection strategies. Here only results for the geometric mean of the three axes of the five largest pumice and lithic clasts collected at both outcrops over specified-area sections are presented in detail (see CTHM-Report for more details). Figure 8 shows the variability of maximum-clast values with sampling area. Values for the largest lithic fragments at outcrop 1 stabilise (i.e. vary by less than ±10 % value, here estimated as the uncertainty in the measure of the clast) around a maximum value for sampling areas larger than 2 m^2, whereas values for pumice fragments of the same outcrop never reach a clear plateau (Fig. 8a). At the same outcrop, the variability of the values measured over several areas of 0.5 m^2 is about 25–30 % (Fig. 8a). Values for both largest pumice and largest lithic clasts of outcrop 2 stabilise around the 0.5-m^2 section (percentage differences <12). Similar to outcrop 1, values measured over areas of 0.2 m^2 show a variability around 25 % (Fig. 8b). The CTHM-Report shows how values for both pumice and lithic fragments at both outcrops never stabilise when collected over unspecified-area sections. It is important to also consider how the characterization of individual clasts is affected by an uncertainty around 10 % (i.e. standard deviation of Fig. 3 and shaded area in Fig. 8).

Table 2 Description of sampling sections of outcrop 1 and 2

Outcrop 1		Outcrop 2	
Specified area	Unspecified area	Specified area	Unspecified area
0.1 m^2 (50×20 cm; α to ε)	A, B (2-m length)	0.1 m^2 (50×20 cm; A to J)	A, B (0.5-m length)
0.5 m^2 (250×20 cm; A to H)	C, D, E (4-m length)	–	C, D, E (1-m length)

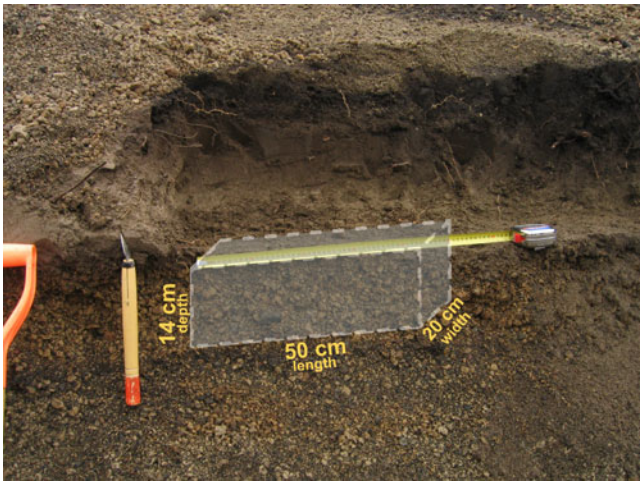

Fig. 4 Example of sampling a specified-area section at outcrop 1 (i.e. 50×20 cm=0.1 m^2). Thickness of the deposit is 14 cm

Discussion and conclusions

The study of the distribution of the largest clasts deposited around a volcano represents one of the most valuable strategies to determine plume height and eruptive style. Nonetheless, our field exercise has shown the strong dependence of the results on different averaging and sampling techniques commonly used in the volcanological literature, confirming the need for a standardised strategy. An important philosophical, but fundamental, concept that needs to be clarified is the idea of the "maximum clast" of an outcrop. This value does not correspond, by definition, to the size of a single clast, but to a representative size obtained by averaging a certain number of the largest clasts collected in a given deposit. The variability of the sample of the largest clasts collected at any given outcrop shows how it would be difficult to define the absolute maximum clast at any location (e.g. Fig. 7). As a result, an outcrop is better characterized by the sample of the largest clasts as opposed to a hypothetical single maximum clast. Suggestions for field procedures and final remarks are summarized below.

Measurement of clast axis

Investigations into the characterization of clast size have shown that the best agreement between an idealized ellipsoid and the measured volume of the clast is given by approximating each clast to the minimum ellipsoid (Fig. 3). Investigators using this technique obtained the best agreement with the diameter of the equivalent sphere, which is what most empirical models for the characterization of tephra deposits are based on (e.g. Carey and Sparks, 1986). In order to ensure the equidimensionality of clasts, we also suggest a shape factor F=0.3 as a plausible threshold for the application of the method of Carey and Sparks (1986) (with F being defined by Wilson and Huang (1979) as $F=(b+c)/2a$). The analysis of shape factor is also important for the choice of averaging technique. If $F \ll 1$, the discrepancy between values obtained using the one-axis techniques (i.e. 1/3 and 1/5) and the three-axes techniques (e.g. 3/5, 3/10, 3/12) are much larger (c.f. Fig. 5). Notably, 1-mm precision is insufficient for clasts <1 cm, in which case we suggest the use of a micron-resolution digital calliper.

Detection of outliers

The dispersal of the largest clasts is related to the dynamics of the convective plume and possibly records both the average behaviour of the plume and its high frequency oscillations. The characterization of the largest clasts should aim at interpreting and evaluating the average behaviour of the plume in order to derive representative eruptive parameters. Clasts which significantly depart from the average values (outliers) should be carefully treated. Clast outliers can be mainly related to density, shape and size. Density outliers are impossible to measure in the field because of the different weight between wet and dry clasts, and shape outliers do not give information on the actual divergence from the assumption of sphere. To overcome density and shape anomalies, analyses should only be ideally carried out on lithic clasts of the same rock type (which are typically characterized by a narrower spread of densities with respect to pumice fragments) and on clasts with F>0.3 (see also previous section). If lithics are characterized by many rock types, the analysis should be carried out on clasts with approximately the same density and certainly clasts characterized by high vesicularity and/or highly altered rocks should be avoided. Nonetheless, the issue of size outliers remains. Given that volcanologists have traditionally dealt with outliers by rejecting them on the basis of subjective criteria, a standard technique should be adopted. Unfortunately, our exercise has shown that both the boxplot method and Dixon's test are not well suited for the evaluation of the largest clast, the former being inappropriate for small populations and the second being too subjective on the size of the sample considered and the assumption of the underlying statistical distribution (see CTHM-Report for more details). A possible reason to exclude outliers could be related, for example, to the presence in the outcrop of clasts that are not in place. Such a possibility needs to be analysed in detail based on outcrop characteristics (e.g. slope, possible slumping and reworking). However, size

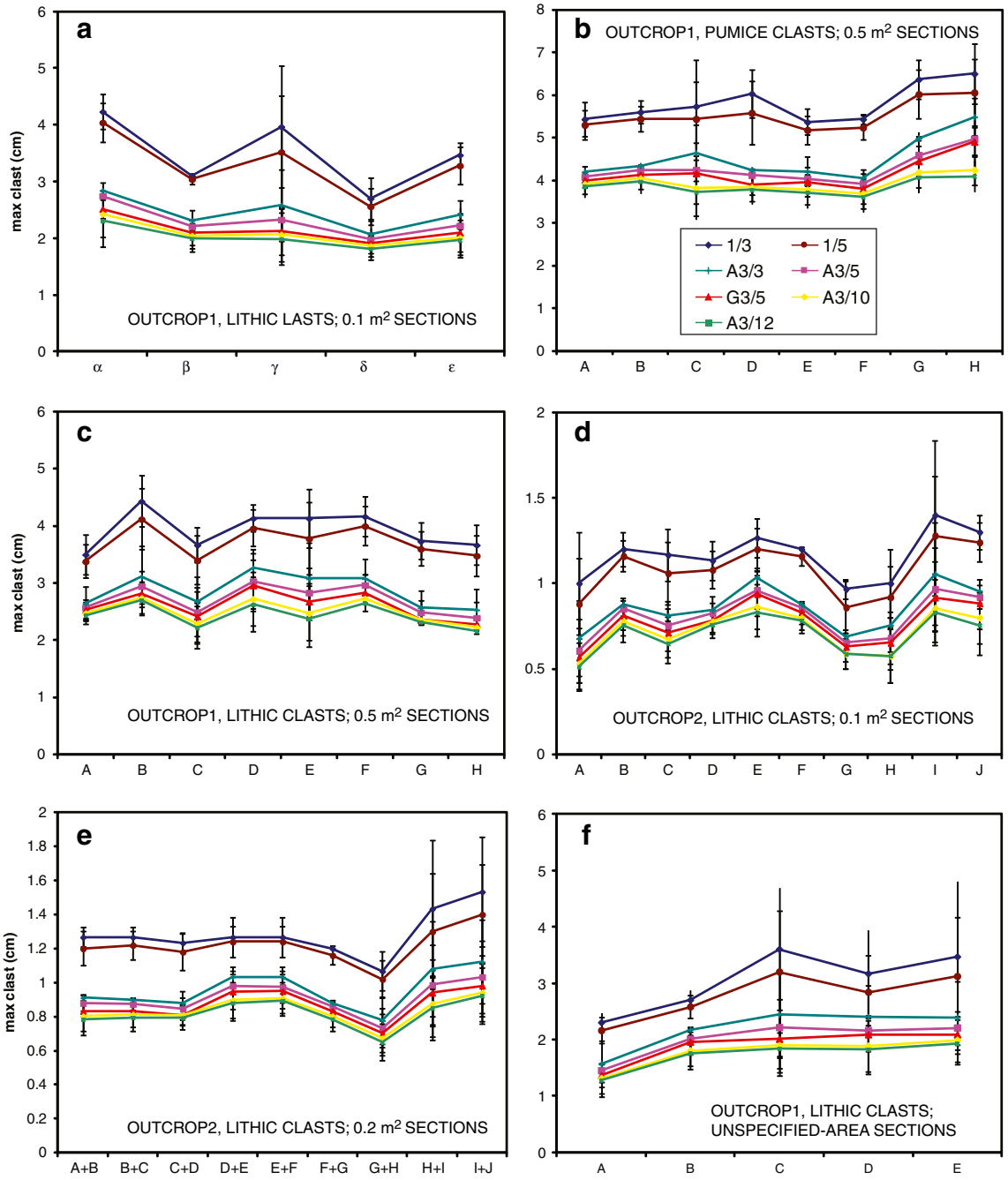

Fig. 5 Variation of the values of the largest pumice and lithic clasts determined using different averaging techniques (described in Table 1) and different sampling areas at the two outcrops: **a** largest lithic clasts collected at outcrop 1 over five specified-area sections of 0.1 m^2 (α to ε); **b** largest pumice clasts collected at outcrop 1 over eight specified-area sections of 0.5 m^2 (A to H); **c** largest lithic clasts collected at outcrop 1 over eight specified-area sections of 0.5 m^2 (A to H); **d** largest lithic clasts collected at outcrop 2 over ten specified-area sections of 0.1 m^2 (A to J); **e** largest lithic clasts collected at outcrop 2 over nine specified-area sections of 0.2 m^2 (derived by coupling two individual areas of 0.1 m^2); **f** largest lithic clasts collected at outcrop 1 over five unspecified-area sections (A to E). Standard deviations for each clast sample are also shown

outliers are also expected to occur due to the inherent variability of the system, e.g. particle diffusion, instability of eruption column. Given such uncertainty in the origin of size outliers, the option of accommodating outliers in order to mitigate their effect on the final results seems more appropriate than rejecting them on a subjective basis. The choice of the 50th percentile of a 20-clast sample represents an alternative strategy to outlier rejection and gave the best results in terms of stability and reproducibility of values (e.g. Fig. 7).

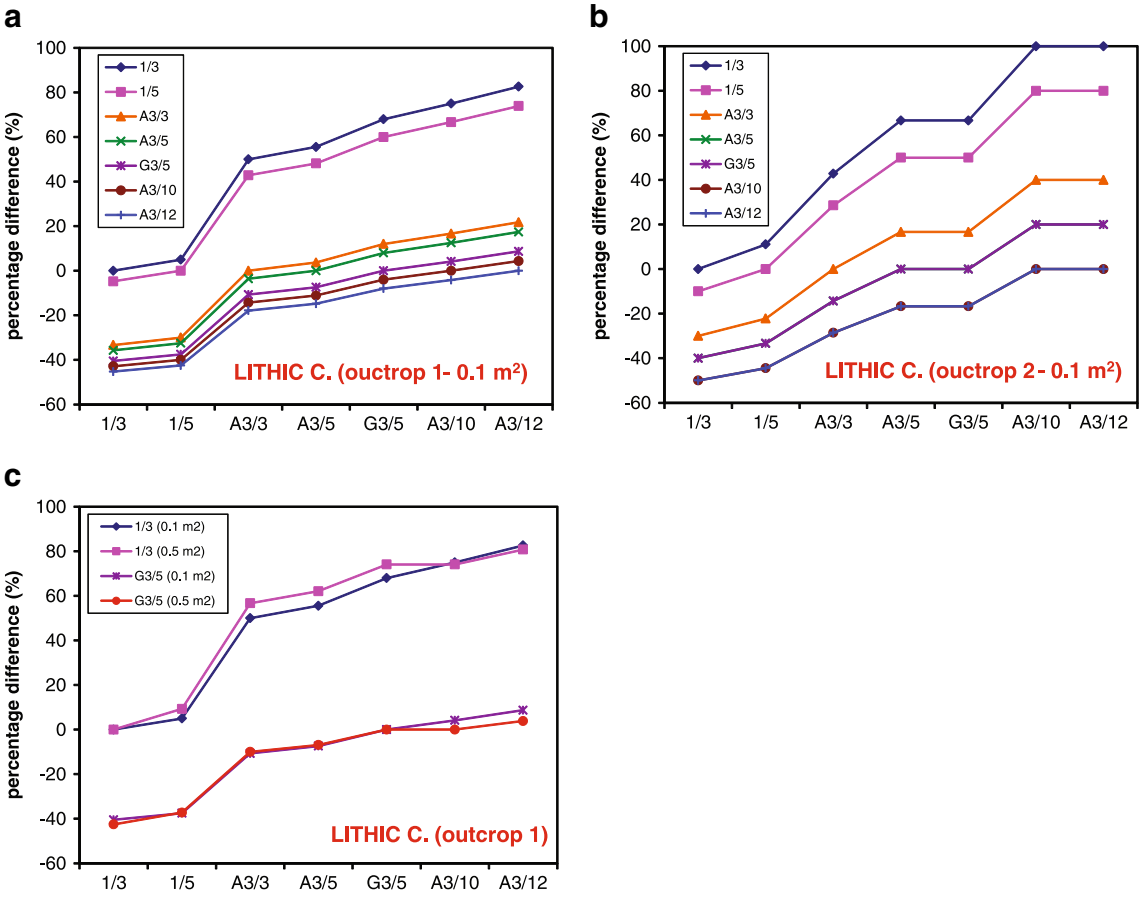

Fig. 6 Percentage difference (considering the formula: $\frac{\text{Value 2}-\text{Value 1}}{\text{Value 1}} \times 100$) amongst different averaging techniques described in Table 1 for lithic clasts of: **a** outcrop 1 and **b** outcrop 2 collected over an area of 0.1 m^2 and **c** comparison between different sampling areas (i.e. 0.1 and 0.5 m^2) at outcrop 1 (please refer to Appendices H and I of the CTHM-Report for more plots and associated data)

Choice of measurement area

Collection strategy: specified-area sections

Our results show that sampling sections up to 1 m^2 for outcrop 1 (Mdϕ=−2.9) and up to 0.2 m^2 for outcrop 2 (Mdϕ=−1.5) are not sufficient to stabilise the data. However, Fig. 8 shows good agreement (i.e. within 10 % uncertainty) between lithic values in the 1 m^2 and 4 m^2 sections of outcrop 1 and both lithic and pumice values in the 0.5- and 1-m^2 sections of outcrop 2. Pumice clasts at outcrop 1 never reach a plateau. In fact, the effect of sampling-area size on the evaluation of the

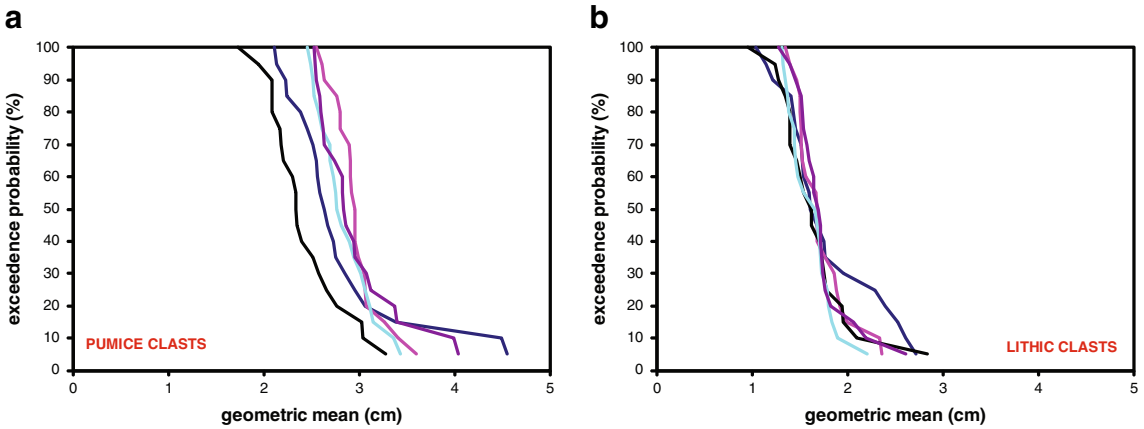

Fig. 7 Empirical survivor plots of geometric mean of three axes of 20 clasts collected over five sampling areas of 0.1 m^2 at outcrop 1: **a** pumice clasts and **b** lithic clasts. Note that results using alternative areas are much more consistent at the 50th percentile than at lower percentiles

Table 3 Comparison of the 50th and 5th percentile for both outcrops. Values are indicated as arithmetic mean ± standard deviation (all data are in Appendix G of the CTHM-Report)

		Pumice clasts	Lithic clasts	Pumice clasts	Lithic clasts
Max axis	50th percentile	3.7±0.3	2.3±0.2	2.4±0.4	0.8±0.2
	5th percentile	5.1±0.8	3.9±0.9	3.7±0.5	1.3±0.2
Geometric mean	50th percentile	2.7±0.2	1.7±0.0	1.7±0.2	0.6±0.1
	5th percentile	3.8±0.5	2.6±0.3	2.7±0.4	0.9±0.2

largest clasts depends on the total grain size distribution of the outcrop investigated. A 0.5-m^2 area is the value suggested by many authors (Fig. 1). In our field exercise, measurements of the largest lithic clasts from the 0.5-m^2 sections of outcrop 1 are ~25 % lower than the stabilised value (4 m^2; Fig. 8a), but the variability measured over several 0.5-m^2 areas is of the same order. A similar difference is observed at outcrop 2 for a 0.2-m^2 measurement area (Fig. 8b), confirming that the area to be measured is dependent on the average grain size of the deposit.

Calibration with grain size and lithic content

The ideal outcrop area to be considered for the collection of the largest lithic clasts depends both on grain size (and hence on Mdϕ) and on lithic content of the size categories larger than the Mdϕ of each outcrop (which are the size categories most representative of the largest clasts). During our exercise, an acceptable stabilization of lithic clast measurements at outcrop 1 (with Mdϕ=−2.9 and an average lithic content of 10 % by volume for the classes larger than the Mdϕ value, i.e. −3ϕ to −5ϕ, Table 4) was reached for a sampled area of 0.5 m^2. Given that the value of a 2D random close packing of spheres is around 0.80 (Delaney et al. 2005), and assuming a monodispersed distribution of particles with diameter equivalent to Mdϕ, i.e. −2.9ϕ, we calculate that a theoretical total value of about 8,000 particles of that diameter would be needed to reach stabilization in the measure of the largest clasts at outcrop 1 (over an area of 0.5 m^2). Based on these assumptions, coloured lines in Fig. 9 represent the minimum area needed to reach stable values for particles similar to those representative of outcrop 1 for different values of Mdϕ and lithic content. This is in good agreement with what we measured at outcrop 2, where the measurements stabilized for a sampling area of 0.2 m^2 (blue circle in Fig. 9).

Choice of averaging technique

Our analysis shows that, first, averaging techniques are not strongly affected by the collection strategy (e.g. Figs 5 and 6 and CTHM-Report). Second, data on the largest clasts carried out at both outcrops show two clear populations of data: one-axis techniques (1/3 and 1/5) and three-axes techniques (A3/5, G3/5, A3/3, A3/10 and A3/12). The percentage difference between the average values of each population (over all averaging techniques considered) varies between 27 and 34 for both pumice and lithic clasts and both outcrops (with an average standard deviation within each population between 0.1 and 0.3 cm). This implies that the results are more sensitive to the choice of number of axes than to the number of clasts considered, particularly when most clasts are characterized by F<0.7 (such as lithic clasts in our case). In addition, given that the model of Carey and Sparks (1986) uses the assumption of spherical particles, the choice of

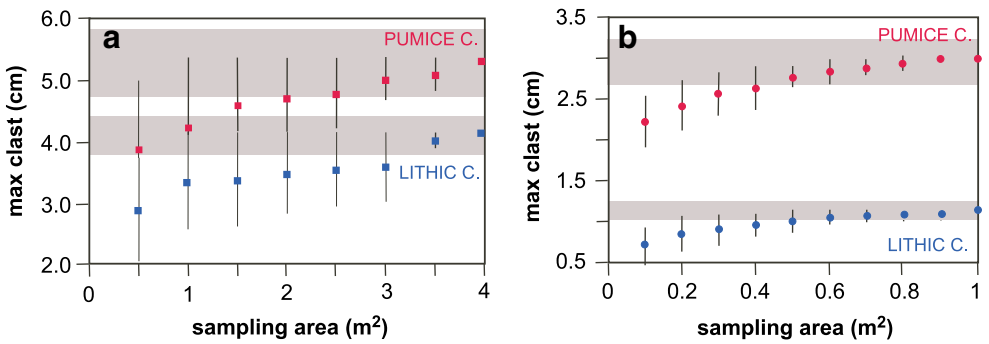

Fig. 8 Variability of maximum-clast measurement with sampling area for the geometric mean of the three axis of the five largest pumice (*red*) and lithic (*blue*) clasts collected at **a** outcrop 1 and **b** outcrop 2. Increasing sampling area is calculated based on the numerical combination of individual sampling area of 0.1 and 0.5 m^2. Bars indicate the variability within individual sampling areas, whereas symbols indicate the mean values (*solid circles* for 0.1-m^2 sampling areas of both outcrop 1 and 2 and *solid squares* for 0.5-m^2 sampling areas of outcrop 1). *Shaded area* indicates the clast-measurement uncertainty estimated in section "Measurement of clast axis" (i.e. 10 %)

Table 4 Number of clasts in 8- to 64-mm size category of a dedicated sample collected at outcrop 1

	Volume	0.013 m^3				
	Pumice clasts		Lithic clasts		Total	
	Weight (g)	Number	Weight (g)	Number	Weight (g)	Number
32–64 mm	31	2	32	1	63	3
16–32 mm	2,094	480	83	12	2,177	492
8–16 mm	4,433	4,362	535	401	4,968	4,763
Total	6,559	4,844	650	414	7,209	5,258

three axes, and, in particular, the choice of the geometric mean of the three axes, is more convenient.

Choice of collection strategy

Clast collection over a 0.5-m^2 depositional area represents a good compromise between data quality and sampling time for both outcrops investigated, and resulting values are typically larger than the values obtained from the unspecified-area sampling on small sections (e.g. Fig. 5). At outcrop 1, the 0.5-m^2 area gives maximum clast measurements about 25 % lower than the stabilised value (corresponding to a 4-m^2 area). A similar result is obtained at the finer-grained outcrop 2 for a 0.2-m^2 area, suggesting that the area to be investigated in order to reach a stabilised value for maximum clasts is dependent on the average grain size of the deposit, as also shown by Fig. 9. This result should be taken into account during field measurements, in order to speed up this time-consuming procedure. We suggest that when the ideal sampling area cannot be excavated (e.g. poorly exposed deposits, archeological sites, densely populated areas), the resulting assessment of the largest clasts needs to be considered as a minimum value. Figure 8 shows the variability of measurement associated with increasing sampling areas for our two outcrops. In particular, 25–30 % uncertainty should be considered when compiling isopleth maps from values of the largest lithics assessed over a 0.5-m^2 area (Fig. 8a). More practically, Fig. 9 could be used to choose the best sampling area according to both grain size and lithic content. It is also important to notice how the uncertainty associated with clast characterization is not negligible (shaded area in Fig. 8).

Characterization of the largest clasts of a given outcrop

We have shown how the values of the largest clasts found at a given outcrop can be plotted based on empirical survivor distributions, and that the 50th

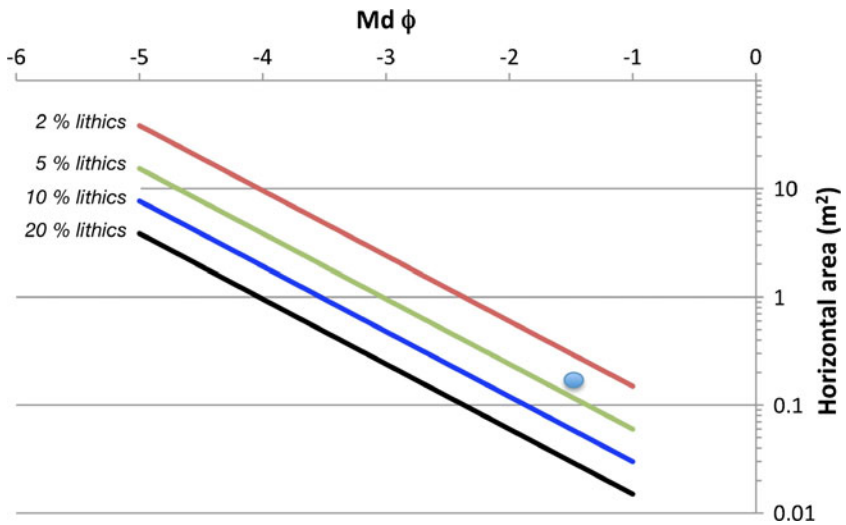

Fig. 9 Dependence of the representative sampling area (i.e. horizontal area of clast deposition) on the outcrop grain size and lithic content. Red line is calculated on the basis of outcrop 1 (Mdϕ=−2.9, lithic content=10%vol., sampling area=0.5 m^2) considering that about 8,000 particles of −3ϕ accumulated over a 0.5-m^2 horizontal surface (based on a close packing of 0.80). Given that the lithic content at outcrop 1 was about 10% volume, we consider that the largest lithic clasts were selected from a total of 800 lithic clasts. Different sampling areas were derived by varying the grain size and the lithic contents (2, 5, 10 and 20% volume) to obtain the same number of particles. The blue circle represents outcrop 2 (Mdϕ=−1.5 and an average lithic content between 2 and 5 % for the classes larger than the Mdϕ value, i.e. −3 and −2)

percentile of these distributions are affected by less variability within the same outcrop than the largest values. The method of the 50th percentile of a 20-largest clast samples described above has the advantages of: (1) eliminating the problem of outlier identification based on a rigorous statistical approach; (2) offering a more reliable reproducibility of the characterization of a given outcrop than the measurement of a small sample of large clasts (e.g. three or five) and (3) reducing analysis time in the field by requiring the detailed measurement of only one clast (i.e. the smallest of the 10 largest clasts). In addition, the underestimation of values is of the same order of magnitude as the differences due to the choice of the collection strategy, sampled volume and averaging technique and can also be corrected when compiling the isopleth map. The model of Carey and Sparks (1986) further developed by Carey and Sigurdsson (1986) and Burden et al. (2011) is based on the comparison between plume vertical velocity and clast terminal velocity, and, therefore, can be used for any clast size. Nonetheless, given that average values of samples of 3, 5, 10 or 12 clasts have been commonly used for the application of these models (Table 1 and Fig. 1), further investigations on the discrepancy between the 50th percentile of a 20-clast sample and more commonly used strategies should be carried out. In fact, the use of the 50th percentile of a 20-clast sample might result in lower but more stable values of plume height with respect to currently used averaging techniques.

Final remarks and suggestions

Suggested field procedures (or best practices) are summarized in Table 5. However, regardless of the method used, it is very important that authors describe in detail the strategy considered for the determination of the maximum clast in order to interpret the associated results (i.e. sampling area/volume and number of clasts and axes considered in the calculation) and facilitate comparison of derived eruption parameters. Given the large discrepancies shown by Fig. 5, we strongly recommend the characterization of three axes of the largest clasts as supposed to the characterization of just one axis. Additionally, the representative sampling area will have to vary based on the lithic content and on the deposit grain size. The uncertainty associated with different averaging techniques and the choice of the best sampling area can be assessed and discussed based on the outcomes of our exercise (Figs. 6 and 9, respectively). Finally, we suggest that future estimates of the maximum clasts are carried out based both on the geometric mean of the three axes of the five largest clasts (G3/5) and on the 50th percentile of an empirical survivor function of a 20-clast sample using the provided template (Electronic supplementary material), and that the results (including the characterization of the 10 largest clasts) be made available to the scientific community. This will generate a large dataset of deposits characterized by different features (e.g. grain size, componentry) that will provide the basis for any future improvement of the assessment of the largest clasts and the modelling of transport and deposition from volcanic plumes.

Table 5 Suggested field procedure

Sampling site
Sections on flat paleotopography far from significant slopes are preferred to sections on sloping paleotopography, because they are likely to be less affected by reworking, slumping and secondary clast grain flows.
Sampling area
Specified-area sections are preferred (i.e. horizontal depositional area; Fig. 4). The plot of Fig. 9 can be used as a rule of thumb to optimize the sampling-section area based on a given outcrop grain size and lithic content. In case sections cannot be excavated, the resulting assessment of the largest clasts has to be considered as a minimum estimate.
Choice of clast to measure
As pumice clasts are generally characterized by a wide range of density and break more easily upon impact with the ground, the characterization of the largest lithic clasts is preferred for the application of the method by Carey and Sparks (1986) (i.e. lithic fragments that are not altered and not highly vesicular). In case of lithic-poor deposits (e.g. basaltic tephra), only the densest juveniles should be used and associated density should be measured.
Clast characterization
Clasts should be characterized based on the geometric mean of its three orthogonal axes with the approximation of the minimum ellipsoid (Fig. 3). Only clasts with $F>0.3$ should be considered in order to avoid large discrepancies with the assumption of spheres.
Choice of largest clasts
The method of the 50th percentile of the 20 largest clast sample is considered as the best way to assess the largest clasts. We recommend the use of the provided template for the determination of the 50th percentile and comparison with the G3/5 technique. Both values should always been determined and reported for future characterizations of tephra deposits.

F is the shape factor of Wilson and Huang (1979) ($F=(b+c)/2a$ with $a>b>c$)

Acknowledgements All workshop participants are especially thanked for their enthusiastic contribution and hard work to collect and characterize a large number of clasts in only 1 day (A. Amigo, D. Andronico, B.L. Browne, K. Bull, R. Carey, K. Cashman, M. Coltelli, L. Connor, L. Costantini, P. Del Carlo, B. Houghton, S. Jenkins, M. Jutzeler, S. Kobs, P. Landi, N. Lautze, C. Magill, C. Melendez Christyanne, C. Principe, F.M. Salani, P. Sruoga, D. Swanson, S. Takarada, A. Volentik, H. Wright). In fact, most data processing to determine the maximum clast was done during the second day of the workshop and preliminary results were discussed with the whole group. Thorough reviews of the Associate Editor V. Manville, S. Sparks and M. Ort have significantly improved the manuscript.

Appendix A

The Dixon's test

The Dixon's test is a convenient and robust statistical test used to identify values that appear divergent from the considered population (Dixon 1950). This technique is recommended for use in small samples (as small as three) and for situations where data are normally distributed but the mean or variance change slowly over time (Chernick 1982). The main limitation is that it requires the assumption of normality (for $n>3$). It is most useful for spotting individual outliers rather than group outliers.

Application The N values comprising the set of observations are arranged in ascending order: $Y_1<Y_2<\ldots<Y_N$. The statistic experimental ratio R_x is calculated based on the observations (where $x=10$, 11, 21 and 22 depending on the population size; Table 6). If $R_x>R_{crit}$, then the suspect value can be characterized as an outlier and it can be rejected. If not, the suspect value must be retained and used in all subsequent calculations. R_{crit} is determined with Table 6 based on population size and critical value α.

Table 6 Critical values for the Dixon test of outliers

n	α 0.1	0.05	0.01	
3	0.886	0.941	0.988	
4	0.679	0.765	0.889	R10=(Y2-Y1)/(Yn-Y1)
5	0.557	0.642	0.780	
6	0.482	0.560	0.698	
7	0.434	0.507	0.637	
8	0.479	0.554	0.683	
9	0.441	0.512	0.635	R11=(Y2-Y1)/(Y(n-1)-Y1)
10	0.409	0.477	0.597	
11	0.517	0.576	0.679	
12	0.490	0.546	0.642	R21=(Y3-Y1)/(Y(n-1)-Y1)
13	0.467	0.521	0.615	
14	0.492	0.546	0.641	
15	0.472	0.525	0.616	
16	0.454	0.507	0.595	
17	0.438	0.490	0.577	
18	0.424	0.475	0.561	R22=(Y3-Y1)/(Y(n-2)-Y1)
19	0.412	0.462	0.547	
20	0.401	0.450	0.535	
21	0.391	0.440	0.524	
22	0.382	0.430	0.514	α is the critical value (10, 5 or 1%)
23	0.374	0.421	0.505	R is the statistical test
24	0.367	0.413	0.497	n is the sample size
25	0.360	0.406	0.489	

References

Aschenbrenner BC (1956) A new method of expressing particle sphericity. J Sediment Petrol 26(1):15–31

Barberi F, Coltelli M, Frullani A, Rosi M, Almeida E (1995) Chronology and dispersal characteristics of recently (last 5000 years) erupted tephra of Cotopaxi (Ecuador): implications for long-term eruptive forecasting. J Volcanol Geotherm Res 69:217–239

Barnett V, Lewis T (1998) Outliers in statistical data. Wiely, Chichester, 584 pp

Biass S, Bonadonna C (2011) A quantitative uncertainty assessment of eruptive parameters derived from tephra deposits: the example of two large eruptions of Cotopaxi volcano, Ecuador. Bull Volcanol 73:73–90

Burden RE, Phillips JC, Hincks TK (2011) Estimating volcanic plume heights from depositional clast size. Journal of Geophysical Research-Solid Earth 116: B11206 doi:10.1029/2011JB008548

Carey SN, Sigurdsson H (1986) The 1982 eruptions of El chichon volcano, Mexico (2): observations and numerical modelling of tephra-fall distribution. Bull Volcanol 48:127–141

Carey S, Sigurdsson H (1987) Temporal variations in column height and magma discharge rate during the 79 AD eruption of Vesuvius. Geol Soc Am Bull 99(2):303–314

Carey SN, Sparks RSJ (1986) Quantitative models of the fallout and dispersal of tephra from volcanic eruption columns. Bull Volcanol 48:109–125

Chernick MR (1982) A note on the robustness of Dixon's ratio test in small samples. Am Stat 36:140

Coltelli M, Del Carlo P, Vezzoli L (1998) Discovery of a Plinian basaltic eruption of roman age at Etna volcano, Italy. Geology 26:1095–1098

Connor LJ, Connor CB (2006) Inversion is the key to dispersion: understanding eruption dynamics by inverting tephra fallout. In: Mader H, Cole S, Connor CB, Connor LG (eds) Statistics in volcanology. Geological Society, London, pp 231–242

Delaney G, Weaire D, Hutzler S, Murphy S (2005) Random packing of elliptical disks. Philosophical Magazine Letters 85(2):89–96

Di Muro A, Rosi M, Aguilera E, Barbieri R, Massa G, Mundula F, Pieri F (2008) Transport and sedimentation dynamics of transitional explosive eruption columns: the example of the 800 BP Quilotoa Plinian eruption (Ecuador). J Volcanol Geotherm Res 174:307–324

Dixon WJ (1950) Analysis of extreme values. Ann Math Stat 21:488–506

Gordon ND, McMahon TA, Finlayson BL (1992) Stream hydrology. An introduction for ecologists. John Wiley and Sons, Chichester, GB

Mastin LG, Guffanti M, Servranckx R, Webley P, Barsotti S, Dean K, Durant A, Ewert JW, Neri A, Rose WI, Schneider D, Siebert L, Stunder B, Swanson G, Tupper A, Volentik A, Waythomas CF (2009) A multidisciplinary effort to assign realistic source parameters to models of volcanic ash-cloud transport and dispersion during eruptions. J Volcanol Geotherm Res 186:10–21

Papale P, Rosi M (1993) A case of no-wind plinian fallout at Pululagua caldera (Ecuador): implications for models of clast dispersal. Bull Volcanol 55:523–535

Pyle DM (1989) The thickness, volume and grainsize of tephra fall deposits. Bull Volcanol 51:1–15

Rosi M, Paladio-Melosantos M, Di Muro A, Leoni R, Bacolcol T (2001) Fall vs flow activity during the 1991 climactic eruption of Pinatubo volcano (Philippines). Bull Volcanol 62:549–566

Scollo S, Tarantola S, Bonadonna C, Coltelli M, Saltelli A (2008) Sensitivity analysis and uncertainty estimation for tephra dispersal models. J Geophys Res 113(B06202)

Shaw DM, Watkins ND, Huang TC (1974) Atmospherically transported volcanic glass in deep sea sediments: theoretical considerations. J Geophys Res 79:3087–3094

Sparks RSJ (1986) The dimensions and dynamics of volcanic eruption columns. Bull Volcanol 48:3–15

Sparks RSJ, Wilson L, Sigurdsson H (1981) The pyroclastic deposits of the 1875 eruption of Askja, Iceland. Philosophical Transaction of the Royal Society of London 229:241–273

Suzuki T, Katsu Y, Nakamura T (1973) Size distribution of the tarumai Ta-b pumice-fall deposit. Bulletin of the Volcanological Society of Japan 18:47–64

Tukey JW (1977) Exploratory data analysis. Addison-Wesley, Reading, MA

Turner JS (1979) Buoyancy effects in fluids. Cambridge University Press, Cambridge, p 368

Walker GPL (1973) Explosive volcanic eruptions—a new classification scheme. Geol Rundsch 62:431–446

Walker GPL, Croasdale R (1971) Two plinian-type eruptions in the Azores. J Geol Soc Lond 127:17–55

Wilson L, Huang TC (1979) The influence of shape on the atmospheric settling velocity of volcanic ash particles. Earth and Planetary Sciences Letters 44:311–324

Wilson L, Walker GPL (1987) Explosive volcanic-eruptions.6. Ejecta dispersal in plinian eruptions—the control of eruption conditions and atmospheric properties. Geophys J R Astron Soc 89:657–679

Woods AW (1988) The fluid-dynamics and thermodynamics of eruption columns. Bull Volcanol 50:169–193

Yuzyk TR, Winkler T (1991) Procedures for bed-material sampling. Lesson package no. 28. Environment Canada, Water Resources Branch, Sediment Survey Section, Ottawa